applied sciences

MDPI

Article

Study of the Stability of Functionalized Gold Nanoparticles for the Colorimetric Detection of Dipeptidyl Peptidase IV

Hasan Aldewachi [1,2,*], Nicola Woodroofe [1] and Philip Gardiner [1]

[1] Biomolecular Sciences Research Centre, Sheffield Hallam University, Sheffield S1 1WB, UK; hwbha2@shu.ac.uk (N.W.); b0037207@my.shu.ac.uk (P.G.)
[2] Department of Pharmaceutical Chemistry, Pharmacy College, Mosul University, Mosul 41001, Iraq
* Correspondence: aldewachi@gmail.com; Tel.: +964-772-118-3160

Received: 24 November 2018; Accepted: 7 December 2018; Published: 12 December 2018

Abstract: In this report, we investigated three stabilization strategies of gold nanoparticles and their practical application for the visual detection of dipeptidyl peptidase IV (DPP-IV). Citrate-capped gold nanoparticles (Au NPs) are generally unstable in high-ionic-strength samples. Au NPs are easily tagged with various proteins and biomolecules rich in amino acids, leading to important biomedical applications including targeted drug delivery, cellular imaging, and biosensing. The investigated assays were based on different modes of stabilization, such as the incorporation of polyethylene glycol (PEG) groups, stabilizer peptide, and bifunctionalization. Although all approaches provided highly stable Au NP platforms demonstrated by zeta potential measurements and resistance to aggregation in a high-ionic-strength saline solution, we found that the Au NPs modified with a separate stabilizer ligand provided the highest stability and was the only platform that demonstrated sensitivity to the addition of DPP-IV, whilst PEGylated and peptide-stabilized Au NPs showed no significant response.

Keywords: gold nanoparticles; stabilization strategies; colorimetric detection; dipeptidyl peptidase IV

1. Introduction

Colloidal gold nanoparticle (Au NP) solutions used in biological assays need to be stable over a wide range of ionic strengths. Therefore, it is essential that attention is paid to the choice of the capping ligands, as these surface bound ligands are responsible for stabilizing NPs against aggregation and providing the desired NP properties (e.g., hydrophilicity/hydrophobicity, surface charge, ligand arrangement, chemical reactivity) [1,2]. A general method of stabilizing Au NPs is the use of electrostatic repulsion between Au NPs, which are modified with charged ligands such as citrate [3] or triphenylphosphine [4]. However, the stability of electrostatically stabilized Au NPs is affected by the solution properties, including pH, ionic strength, and temperature [5].

Several approaches have been developed in order to improve the stability of Au NPs under biological conditions and these generally involve the functionalization of Au NPs with ligands that provide either steric or electrostatic stabilization, thus imparting stability to the Au NP colloid. One of the most commonly used approaches involves the modification of the Au NP surface by assembling a monolayer of peptide-capping ligands [6]. A combinatorial design approach enables the synthesis of ligands that can enhance the stability of the Au NPs in aqueous media [7]. The design strategy of these peptides takes into account the ability of certain amino acid residues to self-assemble into a dense layer that excludes water and a hydrophilic terminus to ensure solubility and stability in water [8]. The aim of this design approach is to produce ligands that, coupled to the Au NPs, will ensure the ligand is bound to the particles through the thiol group on the terminal cysteine.

A different widely applied method is the incorporation of a thiol-containing polyethylene glycol (dithiol-PEG) moiety into the functional ligand, because of its good solubility, biocompatibility, and anti-fouling properties, which render NPs resistant to non-specific protein adsorption [9,10]. A number of workers have utilized functional PEGylated Au NPs in targeted drug delivery and as biosensors in complex media [11–13]. Dougan and colleagues investigated the effect of using multiple thiol linker systems on minimizing undesirable aggregation events caused by thiol desorption, resulting in the loss of function of the probe [14].

Dithiols have also been used because of their higher coupling efficiency to Au NP surfaces, compared to monothiol, which thus enhances the monolayer stability [15,16]. A number of dithiols such as dihydrolipoic acid derivatives [9,17] and di- or polythiol PEGs [18,19] have been assessed for the functionalization of Au NPs in order to impart further stability.

In this report, the effect of incorporating different stabilizer moieties into the assay format was tested for the colorimetric detection of the DPP-IV enzyme (Scheme 1) —a dipeptidase enzyme of high clinical importance, especially as a diagnostic and prognostic marker of various inflammatory disorders, tumors, and hematological malignancies [20,21]—by three distinct methods and was assessed in order to establish the most stable platform that could be exploited for use in high-ionic-strength media such as biological fluids. Table 1 displays the complete sequence of the peptide constructs used in these experiments.

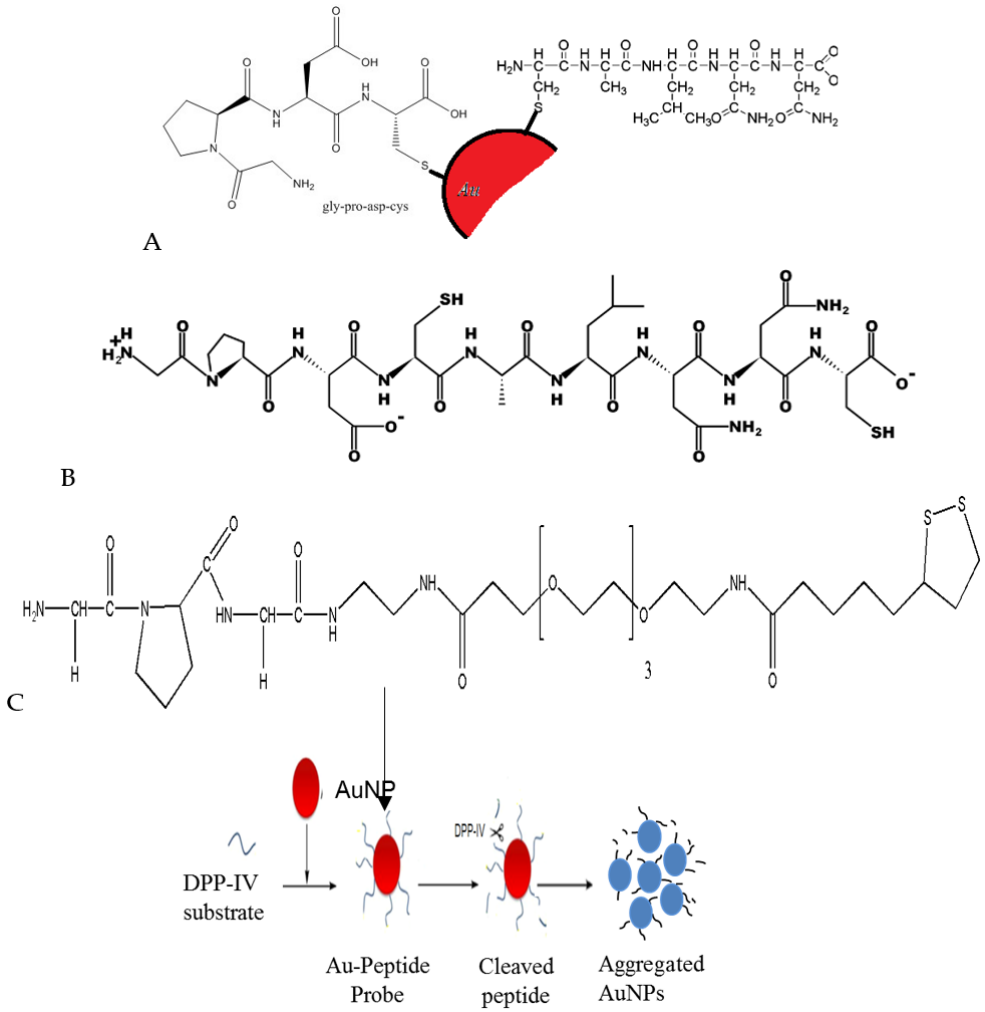

Scheme 1. The mechanism of change of color of the particles. Structure of functional and stabilizer-ligands. (**A**) C/G dipeptide Au NPs, (**B**) GPGCALNNC and (**C**) GPG-EN-PEG4-LA.

Table 1. Peptide sequences trialed to enhance gold nanoparticle (Au NP) stability.

Name	Sequence	Number of Amino Acids
C/G dipeptide	Cys-Ala-Leu-Asn-Asn and Gly-Pro-Asp-Cys	5 and 4
GPG-EN-PEG_4-LA	Gly-Pro-Gly-ethylenediamine-PEG_4-lipoamide	3
GPDCALNNC	Gly-Pro-Asp-Cys-Ala-Leu-Asn-Asn-Cys	9

These approaches were chosen because they are well established in their use in NP systems and they have predictable stability properties [5]. The aim of this study was to enhance the stability of functionalized Au NPs by incorporating stabilizers and to evaluate their effect on DPP-IV detection. It can be clearly observed that the three selected coating ligands differ in their binding moiety and amino acid sequence, which implies a difference in the nanoparticle properties depending on the type of stabilizer used (see Table 2).

Table 2. Summary of ligand and functionalized gold nanoparticle properties.

Ligand Properties			
	C/G dipeptide	GPDCALLNNC	GPG-PEG_4-LA
Binding Moiety	Sulfhydryl	Sulfhydryl	Disulfide
Molecular Weight	390 (GPDC) 533 (CALNN)	906	706
Nanoparticle Properties			
	Au@C/G dipeptide	Au@GPDCALNNC	Au@GPG-PEG_4-LA
Diameter (nm)	14.3 ± 1.1	14.0 ± 1.3	13.8 ± 1.5
λ_{max} ($\Delta\lambda_{max} = \lambda_{max} - \lambda_{original}$)	524.7 (2.9)	524.3 (2.5)	523.5 (1.7)
Hydrated Diameter (nm)	35.4	39.5	38.1
Zeta Potential (mV)	-39 ± 3.5	35.9 ± 1.5	-16.5 ± 1.3

2. Experimental Setup

2.1. Materials

All materials were obtained from suppliers as given below and used as received: DPP-IV enzyme from porcine kidney was purchased from Merck Chemicals (Darmstadt, Germany); hydrogen tetrachloroaurate (III) ($HAuCl_4 \cdot 3H_2O$), 99.99% pure, and sodium citrate dihydrate ($Na_3C_6H_5O_7.2H_2O$), 99% pure, were purchased from Sigma-Aldrich Co. Ltd. (Gillingham, UK) and used without further purification. GPDC (~95% purity) and GPDCALNNC peptide (>90% purity) were purchased from Thermo Fisher Scientific GmbH (Frankfurt, Germany). GPG-ethylenediamine-PEG_4-lipoamide (95% pure) was purchased from Cambridge Research Biochemicals (Cambridge, UK). CALNN peptide (90% pure) was purchased from China peptides (Hangzhou, China).

2.2. Synthesis and Modification of Au NPs with Capping Ligands Preparation

The citrate-stabilized Au NPs were synthesized by using the Grabar method [22]. Briefly, 10 mL of 38.8 mM sodium citrate dihydrate at 50–60 °C were added to 100 mL of 1 mM $HAuCl_4$ under vigorous stirring at boiling point to form a ruby-red-colored solution after a series of color changes. The observed color change was caused by the Surface Plasmon Resonance (SPR) of the forming Au NPs. The solution was cooled to room temperature. The pH was adjusted to 7.4 using 0.5 M NaOH and the solution was filtered through a 0.22 µm pore diameter Millipore syringe filter to remove unreacted salts. The filtrate was stored at 4 °C until required. All glassware and magnetic stirrer bars used in the syntheses were thoroughly cleaned in aqua regia (HCl/HNO_3 3:1, *v*/*v*), rinsed in distilled water, and oven-dried prior to use.

2.2.1. CALNN-, GPDC-Bifunctionalized Au NPs (C/G Au NPs)

C/G Au NPs were prepared by the addition of a peptide mixture (CALNN and GPDC) in various ratios to the solution of Au NPs. GPDC is employed as a functional group which has been evaluated as substrate for DPP-IV [23]; CALNN is used as a stabilizer because pure GPDC-modified Au NPs exhibit poor stability under physiological conditions (ionic strength of 50–200 mM). The stability of C/G-Au NPs is increased by increasing the molar ratio of CALNN to GPDC in the peptide mixture. Bifunctionalized peptide Au NPs were prepared as in the reported procedure with slight modification [9]. Different proportions of CALNN in the ligand shell were obtained by adjusting the ratio of CALNN to GPDC (1:4, 1:6, 1:8, and 1:10) in the peptide mixture. An aqueous solution of peptide mixture (CALNN and GPDC) for each concentration ratio was added to the solution of Au NPs.

2.2.2. Gly-Pro-Gly-Ethylenediamine-PEG_4-Lipoamide (GPG-EN-PEG_4-LA)

In order to use the peptide substrate (GPG-EN-PEG_4-LA), the ring (1,2-dithiolane) has to be opened to form a bidentate thiol anchoring group. Ring opening was achieved by the incubation of the ligand with 50 mM Tris (2-carboxyethyl) phosphine hydrochloride (TCEP) as a reducing agent in a 10:1 (v/v) ratio for 1 hour at room temperature. Functionalized Au NPs were prepared by adding an aqueous solution of PEGylated ligand to the solution of Au NPs.

2.2.3. GPDCALNNC Peptide

Au NPs functionalized with GPDCALNNC peptide were prepared by adding 1 mM peptide solution dissolved in sodium phosphate buffer (pH 7.4) to the solution of Au NPs in a 1:10 (v/v) ratio.

2.3. Purification

The gold conjugates were purified from excess protein and nanoparticles before using them for any experiment or storage. After overnight incubation at room temperature, any excess peptides were removed by two sequential centrifugations (14,500 rpm), each for 15 minutes using a 5415D Eppendorf centrifuge (Eppendorf, Hamburg, Germany). The speed and time were optimized and determined experimentally. The final product was a loose red precipitate. The pellet was resuspended and stored in deionized water at 4 °C.

2.4. Instrumental Techniques

All zeta potential analyses were carried out using the Malvern Zetasizer Nano ZS. The scattered light was detected at a 135° angle with Non-Invasive Backscatter (NIBS) technology. The refractive index of the particle (1.59) polystyrene standard as well as the refractive index (1.33) and the viscosity (0.88) of ultrapure water were measured at 25 °C. All data analyses were performed in automatic mode. The measured size range was presented as the mean value of four runs. For zeta potential measurements, a universal dip cell with an applied voltage of less than 5 V was used and the Smoluchowski approximation was employed by the instrument's software to calculate the zeta potential values for aqueous solutions of Au NPs (F(Ka) value = 1.5).

FTIR spectra were obtained using a PerkinElmer spectrum 100 Fourier Transform Infrared Spectrometer (PerkinElmer, Waltham, MA, USA). The KBr pellet technique is most commonly adopted for recording the spectra. However, in this work, the purified samples were lyophilized and the powdered solid were characterized directly in their free-standing state.

2.5. Assay of DPP-IV/CD26 Activity

To perform the colorimetric assays for DPP-IV/CD26, Aliquots of each modified Au NP preparation were incubated with the enzyme at varying activities in Tris buffer (50 mM, pH 8.3) in the wells of a transparent 96-well microtiter plate. The contents were gently mixed using a plate

shaker at 300–400 rpm for 60 s; and then incubated at 37 °C for 15 min. The UV-vis absorption spectra of the solutions were recorded using absorbance scans from 400 to 900 nm.

3. Results and Discussion

3.1. Investigation of Peptide Coupling Using UV-Visible Spectroscopy

The UV-vis absorption spectroscopy allowed the monitoring of the interaction of the various ligand substrates with Au NPs, since SPR is highly sensitive to the NP environment. The Au NP colloid was found by TEM to be mainly comprised of 14-nm gold spheres exhibiting an extinction maximum at 523–524 nm (Figure 1). Following NP conjugation and coupling reaction with functional ligands (GPDCALNNC or GPG-EN-PEG_4-LA), a slight shift in the absorption maximum was observed between 2.5 and 1.7 nm, respectively, while C/G-modified Au NPs displayed an absorption band shift of 2.9 nm. This shift in λ_{max} of Au NPs was due to the modification of the Au NPs with the various ligands. The coupling of the stabilizing ligands alters the level of the electromagnetic interaction between the Au NPs and the ligand due to the formation of an asymmetric environment. The effect of ligand coupling on the LSPR shift of gold colloids can be accounted for by assuming the contribution of the dielectric of the organic shell [24].

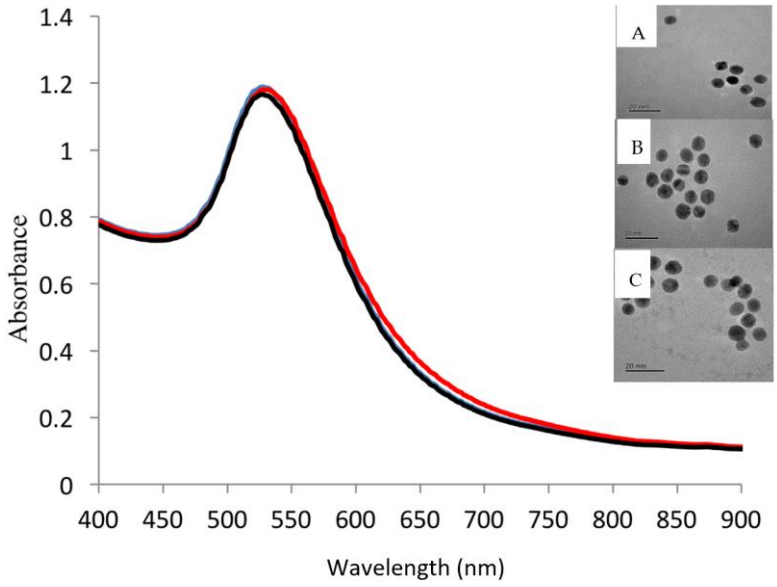

Figure 1. UV-vis absorption spectrum of modified Au NPs. Inset: TEM images (scale bar 20 nm) (black: (**A**) GPDCALNNC-, blue: (**B**) GPG- EN-PEG4-LA-, and red: (**C**) C/G-capped Au NPs).

3.1.1. Evaluation of Ligand Coupling to Gold Nanoparticle Surfaces by FTIR

FTIR spectroscopy was employed to detect changes to the characteristic bands of thiol after Au NP coupling, as free thiol is expected to bind to the Au NP surface via thiolate bonds. Generally, amino acids exist as zwitterions and display spectra featuring both primary amine and carboxylate functional groups. The bands for NH_3^+ stretch (very broad), NH bend (asymmetric/symmetric), and COO^- (carboxylate ion) stretch (asymmetric/symmetric) are typical for this type of compound [24]. In the case of the GPDCALNNC peptide composed of nine amino acids, the main focus was to look for changes in the thiol group in the cysteine. Figure 2 shows the FTIR spectra of the GPDCALNNC before and after coupling to Au NPs. The band in spectrum A at 1652 and 1385 cm^{-1} corresponds to the asymmetric and symmetric stretching of COO^-. A band at 1522 cm^{-1} corresponds to NH bend and the very broad band of NH_3^+ stretch was observed in the 3000–3500 cm^{-1} range. In addition, a weak band near 2550 cm^{-1} confirms the presence of the SH group in the cysteine molecule. These values are in good agreement to those reported by Aryal et al. (2006) for cysteine-capped Au NPs [25].

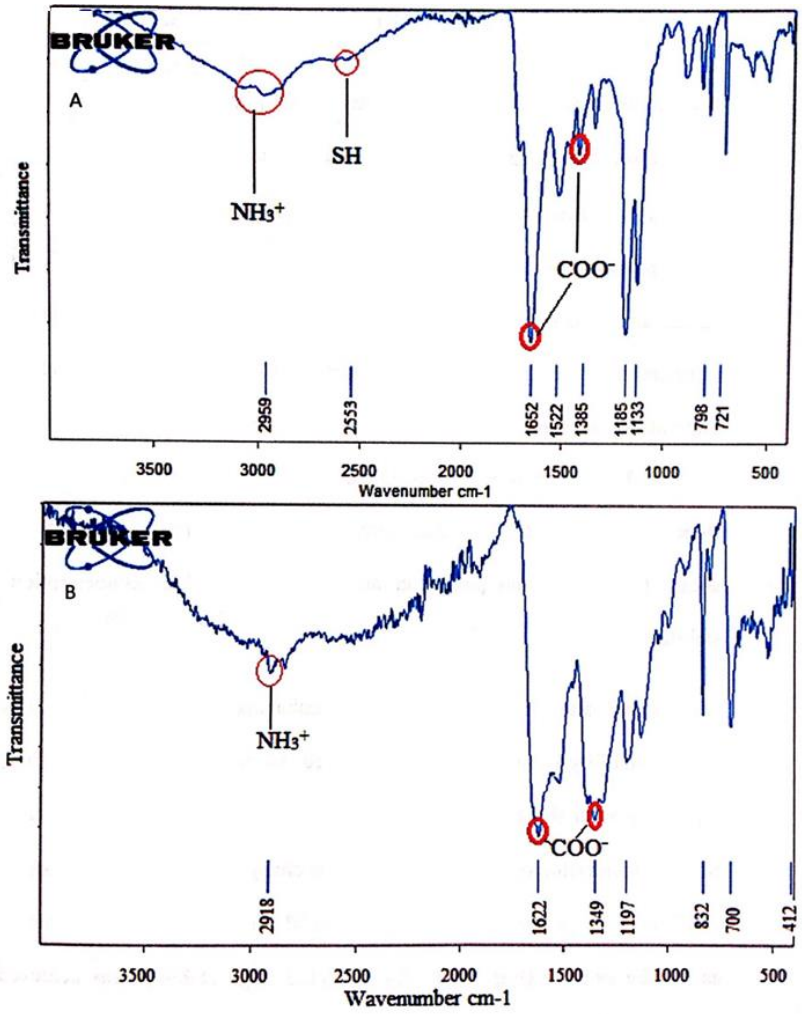

Figure 2. Infrared spectra of stabilized ligand GPDCALNNC (**A**) and GPDCALNNC-capped Au NPs (**B**). Functional ligands inside red circles represent the shift in the band position and disappearance of thiol band, suggesting the formation of a thiolate–gold bond.

These results are in good agreement with the IR spectra of peptides or amino acids, but the characteristic SH band around 2500–2600 cm^{-1} seems to be very weak because of the low levels of sulphur in the peptide. However, small changes in the absorption spectra were detected in the case of GPDCALNN-capped Au NPs (spectra B). A shift in the position of COO^{-} and NH_3^{+} stretching is likely due to a change in their dipole moment, when cysteine binds on a metal surface with high electron density. Although significant band changes due to SH were not observed in the spectra of the free and NP-coupled peptide, other bands of COO^{-} and NH_3^{+} in spectrum B encountered a displacement that may indicate the peptide coupling to the Au NP surface.

3.1.2. Stability of Modified Au NPs in High-Ionic-Strength Solutions

In order to enhance the stability of the Au NP platforms, separate stabilizing ligands were chosen and their stability was evaluated in buffer solutions of varying ionic strengths. The aggregation of Au NPs was used as a means of investigating the stability of the three different platforms (C/G-bifunctionalized ligand, PEGylated ligand, and CALNN-containing ligands). The semi-quantitative measurement of the aggregation process of colloidal NPs was calculated by measuring the variation of the integrated absorbance between 500 and 700 nm [26]. As the absorbance of the Au NP solution shifts to longer wavelengths upon particle aggregation, the flocculation

parameter increases with the extent of particle aggregation. Figure 3A shows the aggregation parameter as a function of NaCl concentration for different stabilizing ligands.

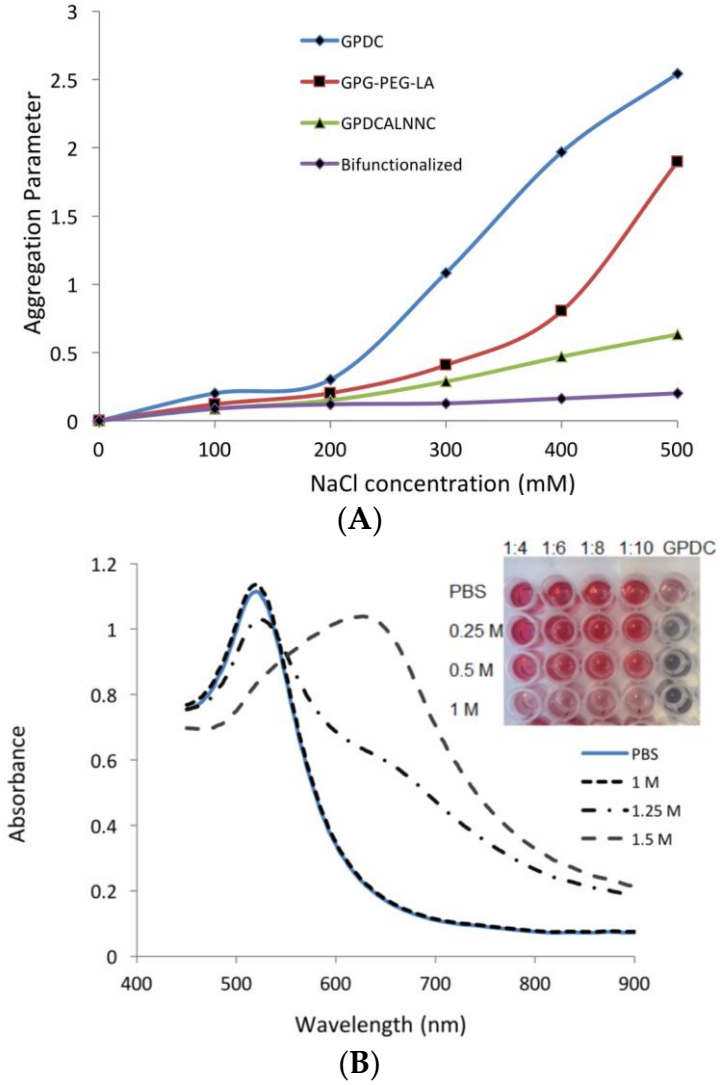

Figure 3. (**A**) Effect of introducing different stabilizing groups on the stability of Au NPs at different ionic strengths. The aggregation parameter is defined as follows: AP = $(A - A_0)/A_0$, where A is the integrated absorbance between 500 and 700 nm of the sample and A_0 is the integrated absorbance between 500 and 700 nm of the initial, fully dispersed solution of NPs. (**B**) UV-vis study of C/G-capped Au NP stability as a function of NaCl concentration. Inset: stability of C/G-capped Au NPs (1:4, 1:6, 1:8, and 1:10) compared to GPDC-capped Au NPs in NaCl solutions with various ionic strengths. As higher concentrations of the salt were added, a greater screening of charges stabilizing the modified Au NPs occurs, leading to the red shift of the absorption band and band broadening.

The incorporation of stabilizing groups enhanced the stability of Au NPs, with the highest stability achieved with the C/G-capped Au NPs. The coupling of CALNN ligand separately with the functional biorecognition ligand offered a stable Au NP up to a NaCl concentration of 1 M, with no evident change in the UV-vis absorbance spectrum. NaCl-induced reversible aggregation [27] occurred at 1.25 M NaCl and was more pronounced at 1.5 M, as can be seen in Figure 3B. As predicted, high stability was achieved due to the formation of a compact self-assembled peptide layer [8].

The other systems investigated were GPDCALNNC-capped NPs and PEGylated ligand tagged with the biorecognition element GP, in which good stability was achieved but to a lesser extent than that obtained by the bifunctionalization of the Au NPs.

3.1.3. Investigation of Zeta Potential and Hydrodynamic Radius

To further assess the stability of the modified Au NP formulations, the zeta potential and average hydrodynamic radius were measured to give further insight into the understanding of the state of the NP surface and to predict the long-term stability of the NP solution. Table 3 summarizes the zeta potential values and hydrodynamic radii of the different functionalized Au NP preparations. The higher negative charge on the surface imparts higher stability owing to the electrostatic repulsion between neighboring particles. The zeta potential values further confirm that the highest stability is achieved with the bifunctionalized Au NP preparation.

Table 3. Average zeta potential and hydrodynamic radius of different peptide-stabilized Au NPs.

Sample	Zeta Potential (mV)	Average Hydrodynamic Radius (nm)
GPDC: CALNN 4:1	−46.1	22.88
GPDC: CALNN 6:1	−38.9	23.68
GPDC: CALNN 10:1	−39.0	35.42
GPDCALNNC	−35.9	39.5
GPG-PEG_4-LA	−16.5	38.1

The stability of C/G-capped Au NPs is improved by increasing the molar ratio of CALNN to GPDC in the peptide mixture, as can be seen in Table 3. The data are in good agreement with the stability noticed in high-ionic-strength solutions. However, it should be noted that the PEGylated ligand displays the lowest zeta potential, which does not coincide with the stability it demonstrates in saline solutions, and this can be interpreted as steric repulsion imparted by coiled PEG, while the zeta potential measures the electrostatic potential that exists between the shear plane of the NPs and the solvent [28].

3.1.4. Detection of DPP-IV Activity Using Functionalized Au NPs

The C/G-capped Au NPs showed a typical SPR peak at 525 nm, i.e., a red shift of 3 nm with respect to the unmodified Au NPs, and good stability in phosphate buffer saline (PBS). After carefully adjusting the molar ratio of CALNN to GPDC, the molar ratio of CALNN to GPDC at 1:10 in the reaction mixture was selected in order to evaluate the sensitivity of the method to DPP-IV/CD26, as this mixture was found to be stable (as shown in Table 3) whilst simultaneously having the highest ratio of bound functional ligand.

A perceptible color change from red to faint purple was only obtained with 15 U/L of DPP-IV activity and it became more evident with increasing the activity to 30 U/L (see Figure 4). The ratio of absorption at 750 and 525 nm was used to evaluate the response of dipeptide-capped Au NPs to DPP-IV/CD26.

Similar conditions were applied to measure DPP-IV/CD26 activity using the PEGylated Au NP system or the GPDCALNNC Au NP system but neither caused color changes, nor was a significant UV-visible spectral shift observed, even at high DPP-IV activities (>50 U/L). This total lack of response was attributed to steric hindrance caused by the compact structure of the remaining ligands (whether PEG or CALNN) bound to the NP and consequently preventing NPs aggregation. A probable reason for the lack of response to DPP-IV/CD26 in the case of GPDCALNNC is the presence of two cysteine residues in the sequence that may form disulphide bridges, leading to a variable percentage of dimerized products [29].

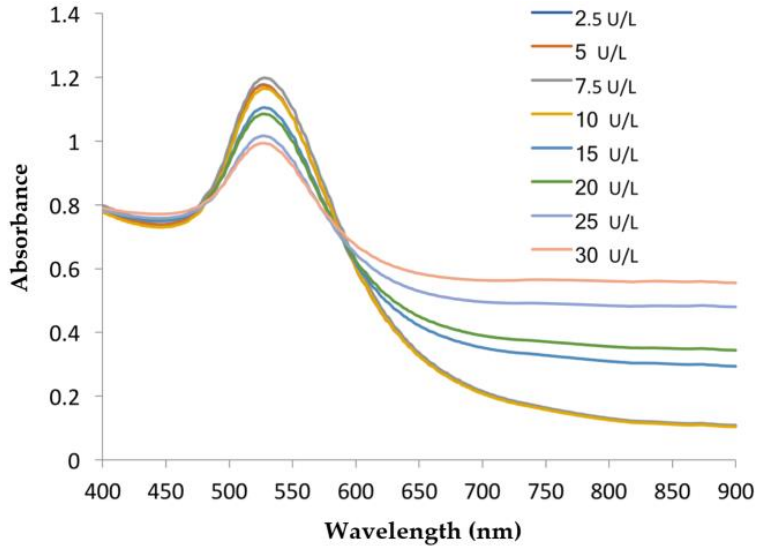

Figure 4. UV-visible absorption spectra of C/G-capped Au NPs after incubation with different activities of DPP-IV/CD26. The DPP-IV/CD26 activity ranged from 10 to 30 U/L. Lower DPP-IV/CD26 activities did not induce spectral changes.

3.1.5. Quantitative Determination of DPP-IV/CD26 Activity

Results of the Au NP assay revealed that the color change was directly proportional to the DPP-IV activity present. The assay provided a quantitative estimation of the total DPP-IV activity in the range of 10–30 U/L. The ratios of spectral absorbance (A_{750}/A_{525}) of the reacted Au NP solutions were plotted as a function of the corresponding standard activities of DPP-IV (U/L). These two absorbance values, A_{750} and A_{525}, were chosen to represent the relative amount of aggregated and dispersed Au NPs, respectively. The increase in the absorbance at 750 nm indicates the formation of the Au NPs clusters/aggregates, while the peak at 525 nm represents the λ_{max} of suspended C/G Au NPs [30,31]. Figure 5 shows that the absorption ratio (A_{750}/A_{525}) of C/G-Au NPs increased with the activity of DPP-IV/CD26 from 10 to 30 U/L.

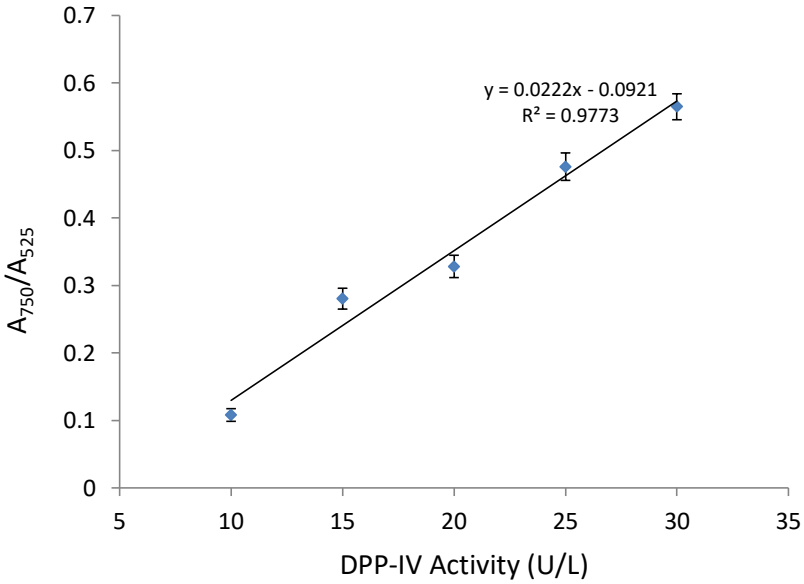

Figure 5. Calibration curve of A_{750}/A_{525} versus the different activities DPP-IV incubated with C/G-capped Au NPs. Error bars represent the standard deviation (n = 3).

4. Conclusions

Three approaches for enhancing modified Au NP system stability were developed and their performances were evaluated. These approaches involved different strategies to enhance the stability of Au NPs for the colorimetric detection of DPP-IV in a high-ionic-strength medium.

The first strategy used the incorporation of a PEGylated sequence with a dithiol anchor because the surface properties of these systems can be engineered through the introduction of functional ligands to create biorecognition ligands [9,32].

The other two strategies used a peptide sequence (CALNN) designed by [8]. This peptide was selected from 58 peptide sequences tested for their high stability and resistance to electrolyte-induced Au NP aggregation. In one strategy, the CALNN peptide was introduced separately as a stabilizer with the previously tested functional ligands, while the third approach involved the decoration of the CALNN peptide with the GPDC ligand.

The stability of these three systems was evaluated against high-ionic-strength solution and exhibited high resistance to aggregation in solutions with up to 0.5 M NaCl, with the highest stability achieved by C/G-capped Au NPs. Further stability studies were conducted by zeta potential measurements. C/G-capped Au NPs displayed the highest zeta potential value, which coincides with its highest stability in saline solution, whilst the PEGylated ligand expressed a low zeta potential value, which might be attributed to the low surface charge of the ligand.

DPP-IV/CD26 activity using the three approaches was detected under optimal conditions and only C/G-capped Au NPs showed a response with a color change when incubated with DPP-IV/CD26. C/G-capped Au NPs were less sensitive than the monofunctionalized systems, with a dynamic range of 10–30 U/L but with very high stability in ionic solutions. This could be attributed to the presence of compact dense layers of CALNN, which hampered effective Au NP aggregation and hence reduced the analytical sensitivity.

In spite of these limitations, the developed bifunctionalized assay was successfully evaluated by gel electrophoresis, zeta potential, and hydrodynamic radius measurements and tested for the assay of DPP-IV activity. These Au NP systems provide insight into different stabilization systems and their effect on the aggregation process. There are a number of parameters to be considered when incorporating a stabilizer, such as the length of the stabilizer residue, the compact density of the stabilizer, and the stabilizer-to-functional ligand ratio [33].

Author Contributions: Conceptualization, P.G. and H.A.; Methodology, H.A.; Validation, P.G., H.A. and N.W.; Formal Analysis, H.A.; Investigation, H.A.; Data Curation, H.A.; Writing—Original Draft Preparation, H.A.; Writing—Review and Editing, H.A.; Visualization, P.G. and N.W.; Supervision, P.G.; Project Administration, P.G. and N.W.

Funding: This research received no external funding.

Conflicts of Interest: The authors declare no conflicts of interest.

References

1. Balasubramanian, S.K.; Yang, L.; Yung, L.Y.L.; Ong, C.N.; Ong, W.Y.; Liya, E.Y. Characterization, purification, and stability of gold nanoparticles. *Biomaterials* **2010**, *31*, 9023–9030. [CrossRef] [PubMed]
2. Zhang, J.J.; Cheng, F.F.; Zheng, T.T.; Zhu, J.J. Versatile aptasensor for electrochemical quantification of cell surface glycan and naked-eye tracking glycolytic inhibition in living cells. *Biosens. Bioelectron.* **2017**, *89*, 937–945. [CrossRef] [PubMed]
3. Martin, M.N.; Basham, J.I.; Chando, P.; Eah, S. Charged gold nanoparticles in non-polar solvents: 10-min synthesis and 2D self-assembly. *Langmuir* **2010**, *26*, 7410–7417. [CrossRef] [PubMed]
4. Ju-Nam, Y.; Bricklebank, N.; Allen, D.W.; Gardiner, P.H.; Light, M.E.; Hursthouse, M.B. Phosphonioalkylthiosulfate zwitterions—New masked thiol ligands for the formation of cationic functionalised gold nanoparticles. *Org. Biomol. Chem.* **2006**, *4*, 4345–4351. [CrossRef] [PubMed]

5. Wang, W.; Wei, Q.; Wang, J.; Wang, B.; Zhang, S.; Yuan, Z. Role of thiol-containing polyethylene glycol (thiol-PEG) in the modification process of gold nanoparticles (AuNPs): Stabilizer or coagulant? *J. Colloid Interface Sci.* **2013**, *404*, 223–229. [CrossRef]
6. Lévy, R. Peptide-Capped Gold Nanoparticles: Towards Artificial Proteins. *ChemBioChem* **2006**, *7*, 1141–1145. [CrossRef] [PubMed]
7. Wang, Z.; Lévy, R.; Fernig, D.G.; Brust, M. Kinase-catalyzed modification of gold nanoparticles: A new approach to colorimetric kinase activity screening. *J. Am. Chem. Soc.* **2006**, *128*, 2214–2215. [CrossRef] [PubMed]
8. Lévy, R.; Thanh, N.T.; Doty, R.C.; Hussain, I.; Nichols, R.J.; Schiffrin, D.J.; Brust, M.; Fernig, D.G. Rational and combinatorial design of peptide capping ligands for gold nanoparticles. *J. Am. Chem. Soc.* **2004**, *126*, 10076–10084. [CrossRef] [PubMed]
9. Eck, W.; Craig, G.; Sigdel, A.; Ritter, G.; Old, L.J.; Tang, L.; Brennan, M.F.; Allen, P.J.; Mason, M.D. PEGylated gold nanoparticles conjugated to monoclonal F19 antibodies as targeted labeling agents for human pancreatic carcinoma tissue. *ACS Nano* **2008**, *2*, 2263–2272. [CrossRef] [PubMed]
10. Manson, J.; Kumar, D.; Meenan, B.J.; Dixon, D. Polyethylene glycol functionalized gold nanoparticles: The influence of capping density on stability in various media. *Gold Bull.* **2011**, *44*, 99–105. [CrossRef]
11. Free, P.S.; Christopher, P.; Lévy, R. PEGylation modulates the interfacial kinetics of proteases on peptide-capped gold nanoparticles. *Chem. Commun.* **2009**, *33*, 5009–5011. [CrossRef] [PubMed]
12. Dreaden, E.C.; Mwakari, S.C.; Sodji, Q.H.; Oyelere, A.K.; El-Sayed, M.A. Tamoxifen-poly (ethylene glycol)-thiol gold nanoparticle conjugates: Enhanced potency and selective delivery for breast cancer treatment. *Bioconjugate Chem.* **2009**, *20*, 2247–2253. [CrossRef] [PubMed]
13. Schiffelers, R.M.; Ansari, A.; Xu, J.; Zhou, Q.; Tang, Q.; Storm, G.; Molema, G.; Lu, P.Y.; Scaria, P.V.; Woodle, M.C. Cancer siRNA therapy by tumor selective delivery with ligand-targeted sterically stabilized nanoparticle. *Nucleic Acids Res.* **2004**, *32*, e149. [CrossRef] [PubMed]
14. Hermanson, G.T. *Bioconjugate Techniques*; Academic Press: Cambridge, MA, USA, 2013.
15. Dougan, J.A.; Karlsson, C.; Smith, W.E.; Graham, D. Enhanced oligonucleotide-nanoparticle conjugate stability using thioctic acid modified oligonucleotides. *Nucleic Acids Res.* **2007**, *35*, 3668–3675. [CrossRef] [PubMed]
16. Susumu, K.; Uyeda, H.T.; Medintz, I.L.; Pons, T.; Delehanty, J.B.; Mattoussi, H. Enhancing the stability and biological functionalities of quantum dots via compact multifunctional ligands. *J. Am. Chem. Soc.* **2007**, *129*, 13987–13996. [CrossRef] [PubMed]
17. Abad, J.M.; Mertens, S.F.; Pita, M.; Fernández, V.M.; Schiffrin, D.J. Functionalization of thioctic acid-capped gold nanoparticles for specific immobilization of histidine-tagged proteins. *J. Am. Chem. Soc.* **2005**, *127*, 5689–5694. [CrossRef] [PubMed]
18. Wang, L.; Wang, L.; Shi, X.; Kariuki, N.N.; Schadt, M.; Wang, G.R.; Rendeng, Q.; Choi, J.; Luo, J.; Lu, S. Array of molecularly mediated thin film assemblies of nanoparticles: Correlation of vapor sensing with interparticle spatial properties. *J. Am. Chem. Soc.* **2007**, *129*, 2161–2170. [CrossRef] [PubMed]
19. Kumar, S.; Aaron, J.; Sokolov, K. Directional conjugation of antibodies to nanoparticles for synthesis of multiplexed optical contrast agents with both delivery and targeting moieties. *Nat. Protoc.* **2008**, *3*, 314–320. [CrossRef] [PubMed]
20. Sun, A.; Deng, J.; Guan, G.; Chen, S.; Liu, Y.; Cheng, J.; Li, Z.; Zhuang, X.; Sun, F.; Deng, H. Dipeptidyl peptidase-IV is a potential molecular biomarker in diabetic kidney disease. *Diabetes Vasc. Dis. Res.* **2012**, *9*, 301–308. [CrossRef] [PubMed]
21. Firnesz, S.F.; Lakatos, P.L. Serum dipeptidyl peptidase IV (DPP IV, CD26) activity in chronic hepatitis C. *Scand. J Gasroenterol.* **2001**, *36*, 877–880. [CrossRef]
22. Grabar, K.C.; Freeman, R.G.; Hommer, M.B.; Natan, M.J. Preparation and characterization of Au colloid monolayers. *Anal. Chem.* **1995**, *67*, 735–743. [CrossRef]
23. Aldewachi, H.S.; Woodroofe, N.; Turega, S.; Gardiner, P.H. Optimization of gold nanoparticle-based real-time colorimetric assay of dipeptidyl peptidase IV activity. *Talanta* **2017**, *169*, 13–19. [CrossRef] [PubMed]
24. Ghosh, S.K.; Pal, T. Interparticle coupling effect on the surface plasmon resonance of gold nanoparticles: From theory to applications. *Chem. Rev.* **2007**, *107*, 4797–4862. [CrossRef] [PubMed]

25. Aryal, S.; Remant, B.K.; Dharmaraj, N.; Bhattarai, N.; Kim, C.H.; Kim, H.Y. Study of electrolyte induced aggregation of gold nanoparticles capped by amino acids. *J. Colloid Interface Sci.* **2006**, *299*, 191–197. [CrossRef] [PubMed]
26. Aryal, S.; Remant, B.K.; Dharmaraj, N.; Bhattarai, N.; Kim, C.H.; Kim, H.Y. Spectroscopic identification of S Au interaction in cysteine capped gold nanoparticles. *Spectrochim. Acta Part A Mol. Biomol. Spectrosc.* **2006**, *63*, 160–163. [CrossRef] [PubMed]
27. Yang, H.; Heng, X.; Wang, W.; Hu, J.; Xu, W. Salt-induced size-selective separation, concentration, and preservation of zwitterion-modified gold nanoparticles. *RSC Adv.* **2012**, *2*, 2671–2674. [CrossRef]
28. Jokerst, J.V.; Lobovkina, T.; Zare, R.N.; Gambhir, S.S. Nanoparticle PEGylation for imaging and therapy. *Nanomedicine* **2011**, *6*, 715–728. [CrossRef] [PubMed]
29. Chen, L.; Annis, I.; Barany, G. Disulfide bond formation in peptides. In *Current Protocols in Protein Science*; Wiley: Hoboken, NJ, USA, 2001; Chapter 18.
30. Chen, G.; Xie, Y.; Zhang, H.; Wang, P.; Cheung, H.Y.; Yang, M.; Sun, H. A general colorimetric method for detecting protease activity based on peptide-induced gold nanoparticle aggregation. *RSC Adv.* **2014**, *4*, 6560–6563. [CrossRef]
31. He, Y.; Cheng, F.; Pang, D.W.; Tang, H.W. Colorimetric and visual determination of DNase I activity using gold nanoparticles as an indicator. *Microchim. Acta* **2017**, *184*, 101–106. [CrossRef]
32. Dixit, V.; Van den Bossche, J.; Sherman, D.M.; Thompson, D.H.; Andres, R.P. Synthesis and grafting of thioctic acid–PEG–folate conjugates onto Au nanoparticles for selective targeting of folate receptor-positive tumor cells. *Bioconjugate Chem.* **2006**, *17*, 603–609. [CrossRef]
33. Lin, S.; Chen, C.; Lin, M.; Hsu, H. A cooperative effect of bifunctionalized nanoparticles on recognition: Sensing alkali ions by crown and carboxylate moieties in aqueous media. *Anal. Chem.* **2005**, *77*, 4821–4828. [CrossRef] [PubMed]